INTERNATIONAL JOURNAL OF Electroactive Materials

*Int. J. Electroactive Mater. 4 (2016) 1 – 7*
*www.electroactmater.com*

# Enhanced Hydrogen Storage Properties of $MgH_2$ by The Addition of $PdCl_2$ Catalyst

**N.S. Mustafa, N. Juahir, F.A. Halim Yap, M. Ismail***

School of Ocean Engineering, Universiti Malaysia Terengganu, 21030 Kuala Terengganu, Malaysia
*E-mails Address: mohammadismail@umt.edu.my

*Received: 22 October 2015 / Accepted: 16 November 2015 / Published: 23 November 2015*

**ABSTRACT:** The effect of $PdCl_2$ on the hydrogen storage properties of $MgH_2$ has been investigated in the present study. The results indicated that the desorption temperature was reduced after the addition of $PdCl_2$ and 20 wt % doping amount showed the best performance in terms of onset dehydrogenation temperature as compared with undoped $MgH_2$. The desorption temperature of $MgH_2$ + 20 wt % $PdCl_2$ was decreased about 275 °C compared to 375 °C and 420 °C for as-milled and as-received $MgH_2$, respectively. The de/rehydrogenation kinetics of the doped $MgH_2$ also improved after doping with $PdCl_2$. From the Kissinger analysis, the apparent activation energy, $E_a$, for hydrogen desorption was reduced from 142 kJ/mol for as-milled $MgH_2$ to 99 kJ/mol after the addition of 20 wt % $PdCl_2$. From the X-ray diffraction result, it is believed that the formation of the new species of $PdH_{0.778}$, $MgCl_2$ and $Mg_6Pd$ during the ball milling or de/rehydrogenation process might actually be responsible for the catalytic effects, and thus, further enhanced the hydrogen storage properties of the $MgH_2$.

**Keywords:** Hydrogen storage, Magnesium hydride, Palladium chloride, Catalytic effect

## 1. Introduction

Hydrogen is expected to play an important role in the future energy economy based on the environmentally clean sources and carriers. However, for the commercialization of hydrogen as a major energy carrier, particularly in the mobile applications, hydrogen suffers from several major drawbacks especially in terms of storage. The storage of hydrogen in solid state widely suggested for the potential solution for compact and safe hydrogen storage for both stationary and mobile applications as a long term alternative. Among the solid state hydrogen storage materials, $MgH_2$ has been considered as a promising hydrogen storage material based on its advantages such as large hydrogen storage capacity (7.6 wt %), good reversibility, low cost and abundant resources [1]. Despite it benefits, the high decomposition temperature and slow desorption/absorption kinetics hinders the use of $MgH_2$ as a hydrogen storage material for practical applications [2, 3]. Many efforts have been done to reduce the decomposition temperature and improve the de/rehydrogenation kinetics of $MgH_2$ such as by ball milling [4, 5] adding with different kind of catalysts [6-14] and causing reaction with other hydrides (destabilized system) [15-18]. Various studies have shown that by adding catalysts, a significant effect on the hydrogenation properties of $MgH_2$ is produced.

So far, however, the effects of metal chloride on the hydrogen storage properties of $MgH_2$ has not been explored as thoroughly as other catalysts such as metal [19-23], metal oxides [24-29], and metal fluorides [12, 30-34] and the state of the metal chloride catalyst and its role were still unclear. Mao et al. [35] reported that by doping $MgH_2$ with $NiCl_2$ or $CoCl_2$, the dehydrogenation temperature and sorption kinetic have been improved. They found that a hydrogen absorption capacity of 5.17 wt % can be reached in 60 s at 300 $^oC$ for the $MgH_2/NiCl_2$ sample while pure $MgH_2$ can just absorb 3.51 wt % hydrogen at 300 $^oC$ in 400 s. From the previous study by Ismail et al. [6] on the effect of $LaCl_3$ on the hydrogen storage properties of $MgH_2$, the results showed that the sample doped with 10 wt % $LaCl_3$ started to decompose at around 300 $^oC$, which was 50 $^oC$ lower than as-milled $MgH_2$. Meanwhile, the onset dehydrogenation temperature of the 10 wt % $FeCl_3$- doped $MgH_2$ sample is reduced by about 90 $^oC$ compared to the as-milled $MgH_2$, and the sorption kinetics measurements indicated that the $FeCl_3$-doped sample displays an average dehydrogenation rate 5-6 times faster than that of the undoped $MgH_2$ sample [36]. All the above studies claim that the improvement of hydrogen storage properties of the $MgH_2$ in the presence of metal chloride due to the catalytic effect of the active species that were form in situ during the heating process. So, it is of interest to further investigate the addition of a different type of metal chloride material and examine the difference in the way they take effect and therefore gain a deeper understanding of the modification of de/rehydrogenation process of $MgH_2$.

In addition, for the best of author's knowledge, no research has been found that surveyed the role of $PdCl_2$ on the hydrogen storage properties of $MgH_2$ alone. However the effect of $PdCl_2$ additive on Mg-25 wt % $Mg_2Ni$ composite has been studied by Wang et al. [37]. They reported that the absorption rate of the composite with $PdCl_2$ was fast and the hydrogen storage capacity was more than that of the composite without $PdCl_2$ which is Mg-25 wt % $Mg_2Ni$-1.5 wt % $PdCl_2$ reacted rapidly with hydrogen at 373 K, the hydriding process was finished within 5 min and the maximum hydrogen storage capacity reached 3.48 wt %. They claimed that $PdCl_2$ dispersed on the surface of Mg-based alloy by ball milling shows

important catalytic effect on the hydrding/dehydring process. In addition, the peaks of $PdCl_2$ or any active species do not appear in the XRD pattern at all conditions. Meanwhile, Bardaji et al. [38] have studied the effects of several metal chlorides on the thermal decomposition behavior of α-$Mg(BH_4)_2$. They found that by using $VCl_3$, $CeCl_3$, $RuCl_3$, $MoCl_3$ and $PdCl_2$ as dopants, the hydrogen desorption of $Mg(BH_4)_2$ can be slightly improved. It also has been reported that the absorption and desorption rates are enhanced for nanocrystalline magnesium powder modified with Pd [39]. Furthermore, from the previous studies by Ismail et al. [40], they believed that the significant improvement in the hydrogen storage properties of $MgH_2$ doped with chlorides of transition metals Hf and Fe is due to the catalytic effect of in-situ generated metal species and $MgCl_2$ that were formed during the dehydrogenation process.

Therefore, in this paper, the effect of ball milled $MgH_2$ doped with $PdCl_2$ is investigated in order to combine the transition metal cations and chlorine anions to prepare for a $MgH_2$-metal chloride system. A pressure-composition-temperature (PCT) apparatus, X-ray diffraction (XRD), differential scanning calorimetry (DSC) and scanning electron microscope (SEM) have been used to investigate their hydrogen storage properties and reaction mechanism.

## 2. Experimental

The $MgH_2$ (98% purity) and $PdCl_2$ (98% purity) were purchased from Sigma-Aldrich and were used as received without pretreatment. All handlings of the powder, including weighing and loading were performed in an argon atmosphere MBraun Unilab glove box. The $MgH_2$, $MgH_2$ + 10 wt % $PdCl_2$ mixture, $MgH_2$ + 20 wt % $PdCl_2$ mixture and $MgH_2$ + 30 wt % $PdCl_2$ were milled in a planetary ball mill (NQM-0.4) for 1 h, by first milling at 15 min, resting for 2 min and then milling for another 15 min with 3 cycles in a different direction at a rotation speed of 300 rpm using hardened stainless steel vials and stainless steel balls. The ratio of the weight of the balls to the weight of the powder was 80:1.

For the temperature-programmed-desorption (TPD) and the rehydrogenation and dehydrogenation kinetic measurements, about 100 mg of the sample was loaded into a sample vessel in the glove box. The experiments were performed in a Sieverts-type pressure-composition temperature (PCT) apparatus (Advanced Material Corporation). For the TPD experiment, all the samples were heated in a vacuum chamber and the amount of desorbed hydrogen was measured to determine the lowest decomposition temperature. The heating rate for the TPD experiment was 5 $^{o}$C/min and samples were heated from 25 $^{o}$C to 450 $^{o}$C. The rehydrogenation kinetics under a hydrogen pressure of 35 atm and the dehydrogenation kinetics under a hydrogen pressure of 1.0 atm were studied at 300 $^{o}$C and 320 $^{o}$C respectively.

Differential scanning calorimetry (DSC) analysis of the dehydrogenation process was carried out on a Mettler Toledo TGA/DSC 1. About 2 – 6 mg of sample was loaded into an alumina crucible in the glove box. The crucible was then placed in a sealed glass bottle in order to prevent oxidation during transportation from the glove box to the DSC apparatus. An empty alumina crucible was used as the reference material. The samples were heated from room temperature to 500 $^{o}$C under an argon flow of 50 mL/min, and different heating rates were used. The microstructures of the samples were characterized by using a scanning electron microscope (SEM; JEOL JSM-6360LA) by setting the samples on carbon tape and then coating them with gold spray under a vacuum. Meanwhile, the phase structures of the samples before and after desorption as well as after rehydrogenation were performed using a Rigaku MiniFlex X-ray diffractometer with Cu Kα radiation. θ-2θ scans were carried out over diffraction angles from 20° to 80° with a speed of 2.00 °/min. All the samples were also prepared in the glove box in order to minimize the oxidation of the sample. To avoid exposure to air during the measurement, the sample was spread uniformly on the sample holder and covered with scotch tape and sealed in plastic wrap.

## 3. Results and Discussion

### 3.1 Dehydrogenation Temperature

**Figure 1** shows the temperature-programmed-desorption (TPD) patterns for the dehydrogenation of as-received $MgH_2$, as-milled $MgH_2$, $MgH_2$ + 10 wt % $PdCl_2$, $MgH_2$ + 20 wt % $PdCl_2$ and $MgH_2$ + 30 wt % $PdCl_2$. The as-received $MgH_2$ started to release hydrogen at about 420 °C, with a total dehydrogenation capacity of 7.42 wt % $H_2$ by 450 °C. After milling, the onset desorption temperature of $MgH_2$ was reduced to about 375 °C with total capacity of hydrogen desorped was about 6.75 wt %, indicating that the milling process also influences the onset desorption temperature of $MgH_2$, as reported by Huot et al. [4].

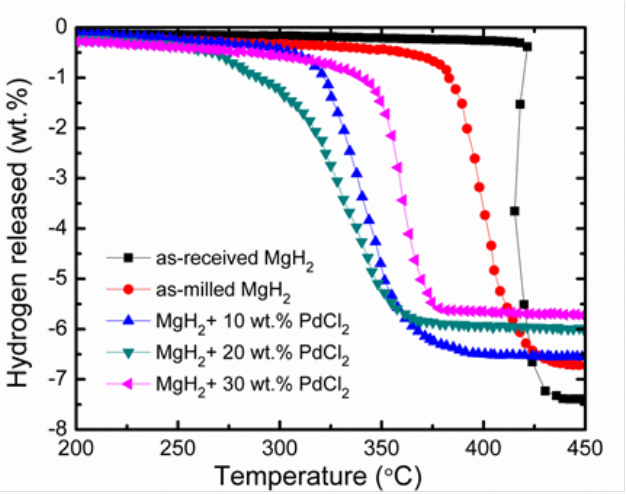


**Figure 1**: The temperature-programmed-desorption (TPD) patterns for the dehydrogenation of as-received $MgH_2$, as-milled $MgH_2$, $MgH_2$ + 10 wt % $PdCl_2$, $MgH_2$ + 20 wt % $PdCl_2$ and $MgH_2$ + 30 wt % $PdCl_2$

After doping with $PdCl_2$, the onset desorption temperature of $MgH_2$ decreased dramatically. The addition of 10 wt % $PdCl_2$ caused decreases in the desorption onset of about 65 °C which is 310 °C. Further increasing the amount of $PdCl_2$ to 20 wt % reduced the onset desorption temperature to 275 °C but the amount of hydrogen released dropped to about 5.7 wt % $H_2$. Meanwhile, after raising the doping amount to 30 wt %, there was more loss of hydrogen released content and the onset desorption temperature was also higher than 10 wt % and 20 wt % which was at about 330 °C.

The reduction of hydrogen capacity after adding the samples with 20 wt % and 30 wt % of $PdCl_2$ may be due to the excessive catalytic effect brought about by the relatively high level of the added $PdCl_2$. This phenomenon was almost the same with our previous paper [9]. However, from the result in **Figure 1** it was shown that the 20 wt % doping amount shows the best performance in terms of onset dehydrogenation temperature. Thus this doping amount is chosen for further analysis.

### 3.2 De/rehydrogenation Kinetics

In order to investigate the performance of the hydrogen desorption kinetics of the $MgH_2$ + 20 wt % $PdCl_2$, the isothermal dehydrogenation kinetic was measured at constant temperature of 320 °C under 1.0 atm pressure as shown in **Figure 2**. The dehydrogenation of $MgH_2$ was also included for comparison purposes. The $MgH_2$ + 20 wt % $PdCl_2$ sample release about 4.4 wt % $H_2$ after 60 min. In contrast, pure $MgH_2$ only releases about 1.2 wt % $H_2$ within the same time. Comparing the two results of the doped samples showed a significant improvement with respect to dehydrogenation kinetic.

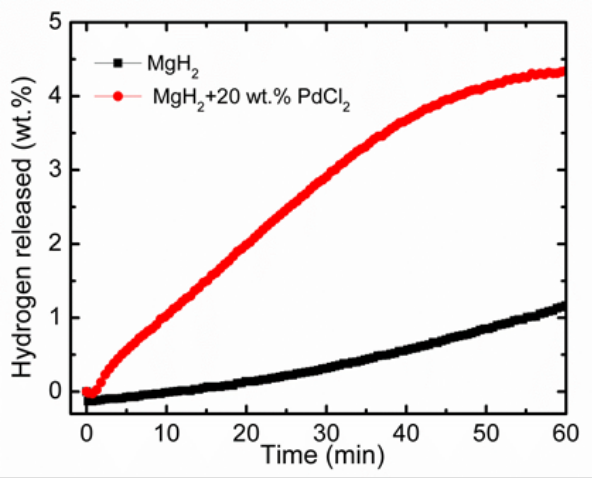


**Figure 2**: Isothermal dehydrogenation kinetic of $MgH_2$ and $MgH_2$ + 20 wt % $PdCl_2$ at 320 °C

**Figure 3** compares the results of the isothermal rehydrogenation kinetics of the as-milled $MgH_2$ and $MgH_2$ + 20 wt % $PdCl_2$ samples at 300 ºC and under 35 atm hydrogen pressure. Although the absorption capacity value for the doped $MgH_2$ sample is less than as-milled $MgH_2$ after 10 min, the sample of 20 wt % $PdCl_2$ doped $MgH_2$ shows faster rehydrogenation kinetic compared to the undoped $MgH_2$. The as-milled $MgH_2$ sample absorbs about 0.9 wt % $H_2$ after 1 min. In contrast, the doped $MgH_2$ sample can absorb about 1.4 wt % $H_2$ within 1 min. Taken together, these results suggest that the rehydrogenation kinetics of $MgH_2$ can also be improved by doping with $PdCl_2$.

### 3.3 Differential Scanning Calorimetry

The thermal properties of as-received $MgH_2$, as-milled $MgH_2$ and $MgH_2$ + 20 wt % $PdCl_2$ were further identified by DSC within the 25 – 500 °C temperature range with the results as shown in **Figure 4**. It can be seen that, the DSC curves for all the samples displayed only one strong endothermic peak which corresponds to the decomposition of $MgH_2$. The DSC curve of as-received $MgH_2$ shows the desorption temperature at approximately 458.56 °C. Meanwhile, the hydrogen desorption temperature for the as-milled $MgH_2$ and $MgH_2$ + 20 wt % $PdCl_2$ shows that the peak of DSC curves has been moved to the lower temperatures as compared with as-received $MgH_2$. The DSC curves for the as-milled $MgH_2$ and $MgH_2$ + 20 wt % $PdCl_2$ samples had strong endothermic peaks at 426.18 °C and 382.74 °C, decreased by approximately 32.38 °C and 75.82 °C, respectively. The reduction of the peak temperature in the DSC result indicated that the dehydrogenation properties of $MgH_2$ were significantly enhanced by adding $PdCl_2$. However, the onset desorption temperatures of the samples from the DSC results were shown slightly higher than TPD. These phenomena may be due to the different atmosphere and heating rates used in the two types of measurements as explained in our previous paper [41-44].

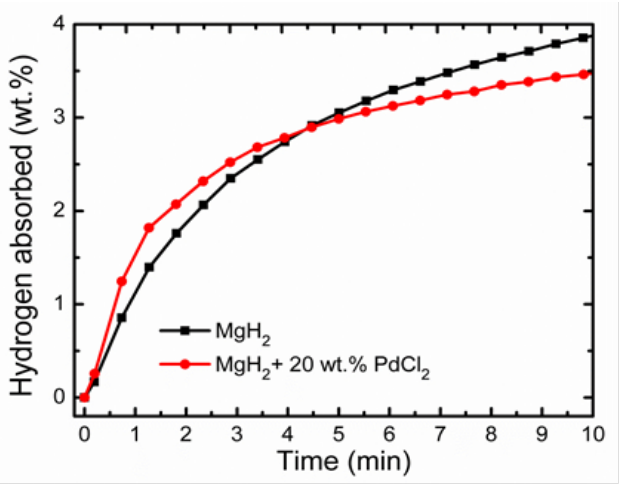


**Figure 3**: Isothermal rehydrogenation kinetic of $MgH_2$ and $MgH_2$ + 20 wt % $PdCl_2$ at 300 °C under 30 atm

In order to determine the effects of $PdCl_2$ addition on the activation energy of MgH2, the Kissinger analysis [45] was used according to the following equation:

$$\ln[\beta/T_p^2] = -E_A/RT_p + A \quad (1)$$

where $\beta$ is the heating rate, $T_p$ is the peak temperature in the DSC curve, $R$ is the gas constant, and $A$ is a linear constant. Thus, the activation energy, $E_A$, could be obtained from the slope in a plot of $\ln[\beta/T_p^2]$ versus $1000/T_p$. **Figure 5** shows the DSC traces at different heating rate for as-received $MgH_2$ **(Figure 5a)**, as-milled $MgH_2$ **(Figure 5b)** and $MgH_2$ + 20 wt % $PdCl_2$ **(Figure 5c)**.

From the Kissinger plot of the DSC data as shown in **Figure 6**, the apparent activation energy, $E_a$, for the as-received $MgH_2$ **(Figure 6a)** and as- milled $MgH_2$ **(Figure 6b)** was found to be 183 kJ/mol and 142 kJ/mol, respectively. After being co-doped with 20 wt % $PdCl_2$ **(Figure 6c)**, the apparent activation energy was lower than as-received and as-milled $MgH_2$, which was reduced by 84 and 43 kJ/mol, respectively (99 kJ/mol). This result indicates that the apparent activation energy has been reduced after doping with $PdCl_2$ and thus helps to improve the dehydrogenation behavior of $MgH_2$.

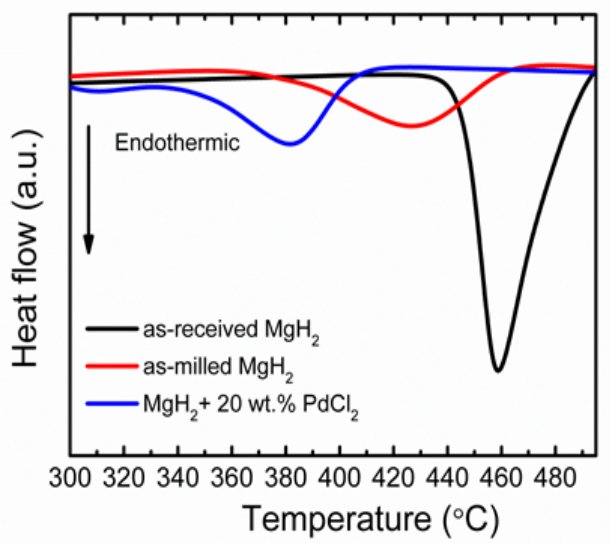


**Figure 4**: DSC traces of as-received $MgH_2$, as-milled $MgH_2$ and $MgH_2$ + 20 wt % $PdCl_2$ (heating rate: 20 °C/min; argon flow: 50 mL/min)

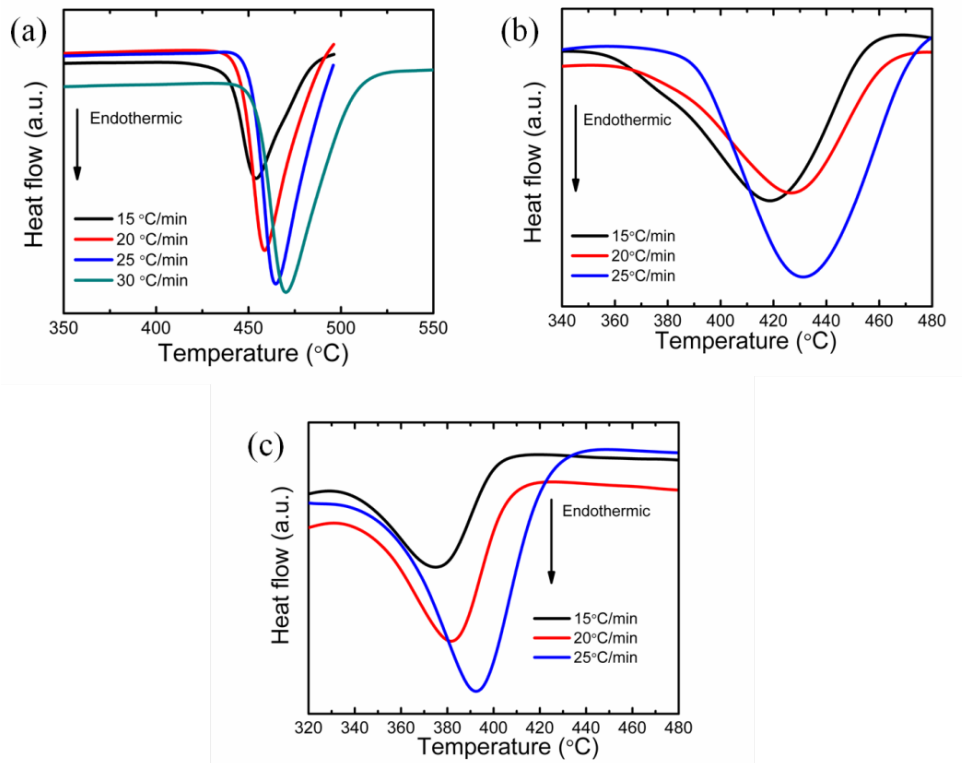


**Figure 5**: DSC traces at different heating rates for (a) as-received $MgH_2$, (b) as-milled $MgH_2$, and (c) $MgH_2$ + 20 wt % $PdCl_2$

### 3.4 Scanning Electron Microscope

**Figure 7** shows the corresponding SEM images of the as-received $MgH_2$, as-milled $MgH_2$ and the as-milled $MgH_2$ + 20 wt % $PdCl_2$. The SEM images illustrated that the particle size of the as-received $MgH_2$ **(Figure 7a)** had an angular shape and the particle size was larger than as-milled $MgH_2$ and $PdCl_2$-doped $MgH_2$ (about 100 µm). Meanwhile, as can be seen from **Figure 7b** the particle size of $MgH_2$ reduced drastically after ball milling for 1 h. However, the particle size was not homogenous and some agglomeration existed in the sample.

In addition, the result indicated that the particle size of $PdCl_2$-doped $MgH_2$ **(Figure 7c)** was smaller than the as-milled $MgH_2$ and appeared to have less agglomeration. It has been reported that the reduction in particle agglomeration and growth resulted in the improvement of the hydrogen storage properties of the light metal hydrides [46]. Meanwhile, a smaller particle size helps to improve

the hydrogen absorption and desorption, because it will reduce the diffusion length and makes the particle surface larger [47]. Hence, it can be speculated that the hydrogen storage properties of $MgH_2$ has been improved after adding the $PdCl_2$ due to the reduction in the particle size and less agglomeration.

### 3.4 X-ray Diffraction

To clarify the phase structure of the doped samples, XRD analysis was performed on the 20 wt % $PdCl_2$ doped $MgH_2$ sample after 1 h ball milling, after dehydrogenation at 450 $^oC$, and after rehydrogenation at 300 $^oC$ under 35 atm, as shown in **Figure 8**. The result shows that after 1 h ball milling **(Figure 8a)**, besides the peaks of $MgH_2$, there was a peak corresponding to the $PdH_{0.778}$ and minor $PdCl_2$ phase existed.

After the dehydrogenation at 450 $^oC$ **(Figure 8b)**, there were distinct peak of Mg, indicating that the dehydrogenation of $MgH_2$ was completed. The transformation of the $MgH_2$ to Mg is represented by the following equation:

$$MgH_2 \rightarrow Mg + H_2 \quad (2)$$

Meanwhile, new diffraction peaks of the $MgCl_2$, $PdH_{0.778}$ and also $Mg_6Pd$ were detected after dehydrogenation process indicating that the reactions of $MgH_2$ and $PdCl_2$ may have occurred and could be postulated as:

$$MgH_2 + PdCl_2 \rightarrow MgCl_2 + PdH_{0.778} + 0.611H_2 \quad (3)$$

$$6MgH_2 + PdH_{0.778} \rightarrow Mg_6Pd + 6.389H_2 \quad (4)$$

For the rehydrogenated sample **(Figure 8c)**, it can be seen that the peak of Mg was largely transformed into $MgH_2$. The peaks of $Mg_6Pd$, $MgCl_2$ and $PdH_{0.778}$ were still present after the rehydrogenated process.

Returning to the results posted above, it is now possible to state that the onset decomposition temperature and de/rehydrogenation kinetic of $MgH_2$ have been improved after the addition of $PdCl_2$. The formation of the $PdH_{0.778}$ particle which resulted from the reaction of the $MgH_2$ and $PdCl_2$ during ball milling and de/rehydrogenation process may play an important role in the enhancement of $MgH_2$ storage properties. On the other hand, the new species of $MgCl_2$ and $Mg_6Pd$ may also introduce an extra catalytic effect on $MgH_2$ sorption properties. From the previous studies it has been reported that the chlorine based product, $MgCl_2$, may contribute to the enhancement of the de/rehydrogenation kinetics by serving as active site for nucleation and creation of the dehydrogenated product by shortening the diffusion distance of the reaction ions [6, 9, 48]. Meanwhile, from the study by Weng et al. [49] on the addition of Pd nanoparticles on the dehydrogenation performance of $LiBH_4/MgH_2$ composite, the result shows the formation of the reaction products of $Mg_6Pd$ and PdH after de/rehydrogenation process. Therefore, the catalytic effect of $PdH_{0.778}$ and $MgCl_2$ may further combine with the catalytic function of $Mg_6Pd$ species to generate a synergetic effect thus further improve the performance of the hydrogen storage properties of $MgH_2$. Since, it was

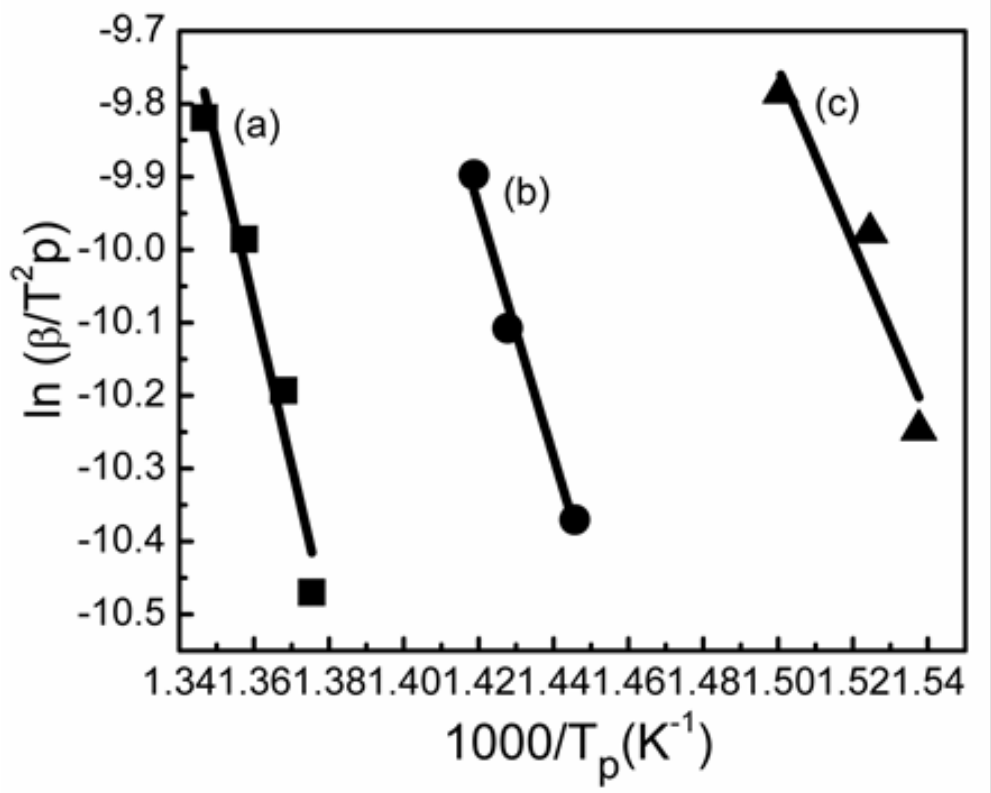


**Figure 6**: Kissinger plot of dehydrogenation for (a) as-received $MgH_2$, (b) as-milled $MgH_2$, and (c) $MgH_2$ + 20 wt % $PdCl_2$

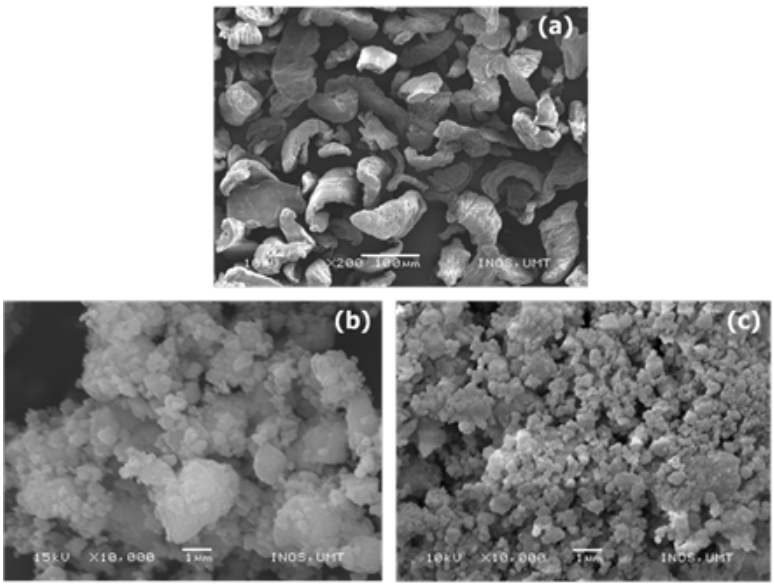


**Figure 7**: SEM micrograph of (a) as-received $MgH_2$, (b) as-milled $MgH_2$, and (c) $MgH_2$ + 20 wt % $PdCl_2$

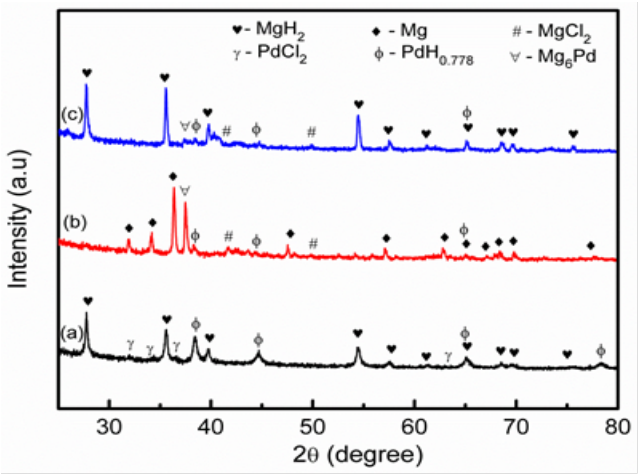


**Figure 8**: XRD patterns of the $MgH_2$ + 20 wt % $PdCl_2$ (a) after milling, (b) after dehydrogenation at 450 °C, and (c) after rehydrogenation at 300 °C

believed that the uses of catalysts can promote the dissociation and recombination of hydrogen at the hydride surface and even added in small amounts can enhance the formation of hydride in reasonable extent [50]. However, in this study the amount of 20 wt % $PdCl_2$ doped with $MgH_2$ showed the best result in onset desorption temperature compared to other amount of $PdCl_2$ doped $MgH_2$.

## 4. Conclusion

The present study was designed to determine the effect of $PdCl_2$ on the hydrogen sorption properties of $MgH_2$. The results of this investigations show that the addition of $PdCl_2$ reduced the onset desorption temperature of $MgH_2$. It can be seen that, 20 wt % doping amount indicates the decreasing of the desorption temperature by 100 °C and 175 °C for as-milled and as-received $MgH_2$, respectively. Thus, this doping amount is chosen for further analysis. Meanwhile, the de/rehydrogenation kinetics of the doped $MgH_2$ was also improved as compared to undoped $MgH_2$. The apparent activation energy calculated from the Kissinger analysis showed the reduction from 142 to 99 kJ/mol after the addition of 20 wt % $PdCl_2$. In addition, the reduction in the particle size and less agglomeration may also help to improve the hydrogen sorption properties of $MgH_2$. It is believed that, the formation of new species of $PdH_{0.778}$, $MgCl_2$ and $Mg_6Pd$ during the ball milling or de/rehydrogenation process might be actually responsible for the catalytic effects, and thus, further improved the hydrogen storage properties of the $MgH_2$.

## Acknowledgement

The authors thank the University Malaysia Terengganu for providing the facilities to carry out this project. The authors also acknowledge the Malaysian Government for the financial support through the Research Acculturation Grant Scheme (RAGS 57087). N. S. Mustafa, N.Juahir, and F.A. Halim Yap are grateful to the Ministry of Education Malaysia for a MyBrain15 scholarship.

## References


1. I.P. Jain, C. Lal, A. Jain, Int. J. Hydrogen Energy 35 (2010) 5133-5144.
2. G. Principi, F. Agresti, A. Maddalena, S. Lo Russo, Energy 34 (2009) 2087-2091.
3. B. Sakintuna, F. Lamari-Darkrim, M. Hirscher, Int. J. Hydrogen Energy 32 (2007) 1121-1140.
4. J. Huot, G. Liang, S. Boily, A. Van Neste, R. Schulz, J. Alloys Compd. 293-295 (1999) 495-500.
5. H. Imamura, K. Tanaka, I. Kitazawa, T. Sumi, Y. Sakata, N. Nakayama, S. Ooshima, J. Alloys Compd. 484 (2009) 939-942.
6. M. Ismail, Energy 79 (2015) 177-182.
7. X.B. Yu, Y.H. Guo, H. Yang, Z. Wu, D.M. Grant, G.S. Walker, J. Phys. Chem. C 113 (2009) 5324-5328.
8. F.A. Halim Yap, N.S. Mustafa, M. Ismail, RSC Adv. 5 (2015) 9255-9260.
9. M. Ismail, Int. J. Hydrogen Energy 39 (2014) 2567-2574.
10. X.B. Yu, Z.X. Yang, H.K. Liu, D.M. Grant, G.S. Walker, Int. J. Hydrogen Energy 35 (2010) 6338-6344.
11. N.S. Mustafa, M. Ismail, Int. J. Hydrogen Energy 39 (2014) 15563-15569.
12. I.E. Malka, M. Pisarek, T. Czujko, J. Bystrzycki, Int. J. Hydrogen Energy 36 (2011) 12909-12917.
13. H.B. Lu, C.K. Poh, L.C. Zhang, Z.P. Guo, X.B. Yu, H.K. Liu, J. Alloys Compd. 481 (2009) 152-155.
14. A. Ranjbar, M. Ismail, Z.P. Guo, X.B. Yu, H.K. Liu, Int. J. Hydrogen Energy 35 (2010) 7821-7826.
15. Y. Zhang, Q.-F. Tian, S.-S. Liu, L.-X. Sun, J. Power Sources 185 (2008) 1514-1518.
16. Mustafa NS, Ismail M, Int. J Hydrogen Energy 39 (2014) 7834-7841.
17. M. Ismail, Y. Zhao, X.B. Yu, S.X. Dou, RSC Adv. 1 (2011) 408-414.
18. M. Ismail, Y. Zhao, X.B. Yu, S.X. Dou, Int. J. Hydrogen Energy 37 (2012) 8395-8401.
19. C.X. Shang, M. Bououdina, Y. Song, Z.X. Guo, Int. J. Hydrogen Energy 29 (2004) 73-80.
20. J.L. Bobet, E. Akiba, Y. Nakamura, B. Darriet, Int. J. Hydrogen Energy 25 (2000) 987-996.
21. G. Liang, J. Huot, S. Boily, A. Van Neste, R. Schulz, J. Alloys Compd. 292 (1999) 247-252.
22. H. Gasan, O.N. Celik, N. Aydinbeyli, Y.M. Yaman, Int. J. Hydrogen Energy 37 (2012) 1912-1918.
23. S.-k. Peng, X.-z. Xiao, R.-j. Xu, L. Li, F. Wu, S.-q. Li, Q.-d. Wang, L.-x. Chen, T. Nonferr. Metal Soc. 20 (2010) 1879-1884.
24. M. Polanski, J. Bystrzycki, J. Alloys Compd. 486 (2009) 697-701.
25. O. Friedrichs, J.C. Sanchez-Lopez, C. Lopez-Cartes, T. Klassen, R. Bormann, A. Fernandez, J. Phys. Chem. B 110 (2006) 7845-7850.
26. G. Barkhordarian, T. Klassen, R. Bormann, Scripta Mater. 49 (2003) 213-217.
27. D.L. Croston, D.M. Grant, G.S. Walker, J. Alloys Compd. 492 (2010) 251-258.
28. V.V. Bhat, A. Rougier, L. Aymard, X. Darok, G. Nazri, J.M. Tarascon, J. Power Sources 159 (2006) 107-110.
29. V.V. Bhat, A. Rougier, L. Aymard, G.A. Nazri, J.M. Tarascon, J. Alloys Compd. 460 (2008) 507-512.
30. S.-A. Jin, J.-H. Shim, Y.W. Cho, K.-W. Yi, J. Power Sources 172 (2007) 859-862.
31. I.E. Malka, T. Czujko, J. Bystrzycki, Int. J. Hydrogen Energy 35 (2010) 1706-1712.
32. J.F.R.d. Castro, A.R. Yavari, A. LeMoulec, T.T. Ishikawa, W.J.B. F, J. Alloys Compd. 389 (2005) 270-274.
33. L. Xie, Y. Liu, Y.T. Wang, J. Zheng, X.G. Li, Acta Mater. 55 (2007) 4585-4591.
34. A.R. Yavari, A. LeMoulec, F.R. de Castro, S. Deledda, O. Friedrichs, W.J. Botta, G. Vaughan, T. Klassen, A. Fernandez, Ç. Kvick, Scripta Mater. 52 (2005) 719-724.
35. J. Mao, Z. Guo, X. Yu, H. Liu, Z. Wu, J. Ni, Int. J. Hydrogen Energy 35 (2010) 4569-4575.
36. M. Ismail, Int. J. Hydrogen Energy 39 (2014) 2567-2574.
37. X.L. Wang, J.P. Tu, P.L. Zhang, X.B. Zhao, J. Zhejiang Univ. - Sci. A 8 (2007) 1510-1513.
38. E.G. Bardají, N. Hanada, O. Zabara, M. Fichtner, Int. J. Hydrogen Energy 36 (2011) 12313-12318.
39. A. Zaluska, L. Zaluski, J.O. Ström–Olsen, J. Alloys Compd. 288 (1999) 217-225.
40. M. Ismail, Y. Zhao, X. Yu, S. Dou, Energy Edu. Sci. Technol. Part A Energy Sci. Res. 30 (2012) 107-122
41. M. Ismail, Y. Zhao, X.B. Yu, S.X. Dou, Int. J. Hydrogen Energy 35 (2010) 2361-2367.
42. M. Ismail, Y. Zhao, X.B. Yu, A. Ranjbar, S.X. Dou, Int. J. Hydrogen Energy 36 (2011) 3593-3599.
43. M. Ismail, Y. Zhao, X.B. Yu, I.P. Nevirkovets, S.X. Dou, Int. J. Hydrogen Energy 36 (2011) 8327-8334.
44. M. Ismail, Y. Zhao, X.B. Yu, S.X. Dou, Int. J. Electroactive Mater. 1 (2013) 13-22.
45. H.E. Kissinger, Anal. Chem. 29 (1957) 1702-1706.
46. M. Ismail, N. Juahir, N.S. Mustafa, J. Phys. Chem. C 118 (2014) 18878-18883.
47. A. Ranjbar, Z.P. Guo, X.B. Yu, D. Wexler, A. Calka, C.J. Kim, H.K. Liu, Mater. Chem. Phys. 114 (2009) 168-172.
48. F. Zhai, P. Li, A. Sun, S. Wu, Q. Wan, W. Zhang, Y. Li, L. Cui, X. Qu, J. Phys. Chem. C 116 (2012) 11939-11945.
49. B.C. Weng, X.B. Yu, Z. Wu, Z.L. Li, T.S. Huang, N.X. Xu, J. Ni, J. Alloys Compd. 503 (2010) 345-349.
50. J.C. Crivello, T. Nobuki, T. Kuji, Int. J. Hydrogen Energy 34 (2009) 1937-1943.